Electronic Supplementary Information (ESI)

Nanoporous organic polymer using 1, 3-dibromoadamantane as a crosslinker for adsorption/separation of benzene and cyclohexane

Jun Yan,*[a,b] Jiangli Zhu,[a,b] SihanTong,[a,b] and Zefeng Wang*[c,d]

[a]*School of Materials Science and Engineering, North Minzu University, Yinchuan 750021, China*

[b]*International Scientific and Technological Cooperation Base of Industrial Solid Waste Cyclic Utilization and Advanced Materials, Yinchuan 750021, China*

[c]*College of Ecology, Lishui University, Lishui 323000, China*

[d]*R&D Center of Green Manufacturing New Materials and Technology of Synthetic Leather Sichuan University-Lishui University, Lishui 323000, China*

Corresponding Authors:

Dr. Jun Yan; Email: yanjun2018@nun.edu.cn；

Dr. Zefeng Wang; Email:shangk72@163.com;

Expermental Section

Materials

1, 3-dibromoadamantane (DBAd), hexaphenylbenzene (HPB), tetrahydrofuran (THF), dichloromethane (DCM) (99.9%, Superdry), and N, N-dimethyformamide (DMF) were purchased from J&K Chemical Co., Ltd and used as received.

Synthesis of NOP-Ad-1

Under a flow of N_2, a dry 50 ml Schlenk flask was filled with DBAd (0.88 g, 3.0 mmol), HPB (0.53 g, 1.0 mmol), $AlCl_3$ (0.95 g, 7.2 mmol), and DCM (10.0 ml). The mixture was stirred at 40°C for 12 hours. Once the reaction reached completion, the system was allowed to cool naturally to room temperature. The resulting solid was separated by filtration and sequentially washed with 1 M HCl, deionized water, DMF, DCM, and THF. Finally, the resulting solid was extracted with THF using a Soxhlet apparatus for 3 days and dried in a vacuum oven at 120°C for 48 hours, yielding 98%.

Material characterization

The morphology of the samples was evaluated by field-emission scanning electron microscopy (FE-SEM; SUPRATM 55). The chemical structure of the synthesized polymers was characterized via Fourier transform infrared (FTIR) spectroscopy performed on a Nicolet 20XB FTIR spectrophotometer in the wavenumber range of 400-4000 cm^{-1}. The synthesized polymers were also dispersed in KBr to form disks for capturing solid-state nuclear magnetic resonance (NMR) spectra. ^{1}H NMR spectra were collected using a 400 MHz Varian INOVA NMR spectrometer using tetramethylsilane (TMS) as an internal standard. Solid-state ^{13}C NMR spectra were recorded in conjunction with the cross-polarization (CP) and total suppression of spinning sidebands (TOSS) techniques on a Bruker AVANCE III HD 600 MHz Ascend Wide-Bore NMR spectrometer. Elemental analyses (EA) were conducted on Elementar Vario EL III. Powder Wide-angle X-ray diffractions (WAXD) data from 5°to 60° were collected using a Rigku D/max-2400 X-ray diffractometer (40 kV, 200 mA) with a copper target at a scanning rate of 2°/min. Thermogravimetric analysis (TGA) curves were recorded on a NETZSCH TG 209 thermal analyzer

by heating the samples (~8 mg) from room temperature to 800°C with a heating rate of 10°C/min under an N_2 atmosphere.

The C_6H_6 and C_6H_{12} adsorption and desorption characteristics of the synthesized polymers were analyzed using an Autosorb iQ2 gas sorption analyzer (Quantachrome Instruments). Prior to testing, the polymers were degassed overnight at 100°C under high vacuum. The specific surface areas (S_{BET}) of the synthesized polymers were calculated based on the Brunauer-Emmett-Teller (BET) model on the basis of N_2 adsorption and desorption isotherms obtained at 77 K. These isotherms were also subjected to analysis based on non-local density function theory (NLDFT) to determine the pore size distributions of the polymer samples. In addition, the micropore surface area (S_{micro}) and micropore volume (V_{micro}) were calculated by the t-plot method, and the total pore volume (V_{total}) was determined from the N_2 adsorption isotherms at a relative pressure of P/P_0 = 0.99.

The adsorption separation performance of mixed gas was tested by a multi-component adsorption penetration curve analyzer. The inner diameter of the sample tube is 5 mm and the length is 20 cm. Degassing treatment before test: The sample was degassed with helium (50 mL/min) purge mode, and the sample was heated to 120℃ for 2 hours. The test temperature of the sample was maintained at 298 K during the test. Helium controls the ratio series of benzene and cyclohexane as 20:80, 35:65, 50:50, 65:35, and 80:20, and the total flow rate of mixed gas is approximately 15 mL/min. The gas composition was obtained by GC test.

$$Q_{nad} = Q_{min} - Q_{nout} = q_{in} \times c_{no}\Delta T - \int_0^t [(q/(1-\sum_1^N C_{nt}))]C_{nt} \, dt \quad \text{(formula 1)}$$

The adsorption capacity of the adsorbent is calculated according to formula 1: Where Q_{nad} represents the adsorption capacity of the adsorbent n, Q_{min} represents the total flow rate of the adsorbent "n" entering the penetration column at ΔT, Q_{nout} represents the total flow rate of the adsorbent n flowing out of the penetration column at ΔT, q_{in} represents the total flow rate of the gas through the entrance of the penetration column, c_{no} represents the total flow rate of the gas through the exit of the penetration column, ΔT represents the total adsorption time. "q" is the flow rate of carrier gas, C_{nt} is the concentration percentage of adsorbent at the entrance of the penetrating

column.

$$s = \left(\frac{x_1}{y_1}\right) \div \left(\frac{x_2}{y_2}\right) \quad \text{(formula 2)}$$

The selectivity of gas 1 to gas 2 is calculated according to formula 2: X_1/Y_1 represents the adsorption phase molar fraction of component 1 gas phase adsorption phase molar fraction, X_2/Y_2 represents the adsorption phase molar fraction of component 2 gas phase adsorption phase molar fraction.

The Ideal Bz/Cy selectivity S :

$$s = \left(\frac{U_1}{y_1}\right) \div \left(\frac{U_2}{y_2}\right) \quad \text{(formula 3)}$$

$$y_1 + y_2 = 1 \quad \text{(formula 4)}$$

The selectivity of benzene 1 to cyclohexane 2 is calculated using formula 3. In this formula, U_1 represents the benzene uptake at the adsorption phase molar fraction y_1, while U_2 represents the cyclohexane uptake at the adsorption phase molar fraction y_2.

Computational details

A first-principles electronic structure investigation of the NOP-Ad-1 fragment was conducted using the density functional theory (DFT) computational approach. Geometry optimization of the structures of NOP-Ad-1 fragment was achieved utilizing the ωB97XD functional along with Gaussian 03 and GaussView computational packages. The geometry optimization employed a basis set of 6-311++(d, p).

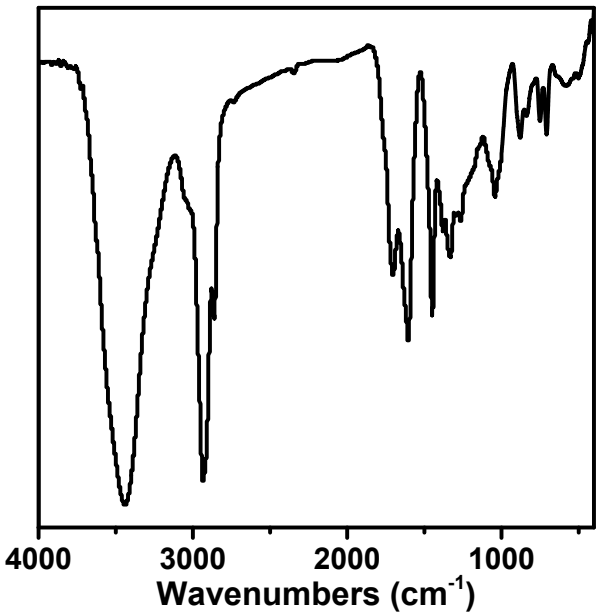

Figure S1. FTIR spectra of NOP-Ad-1.

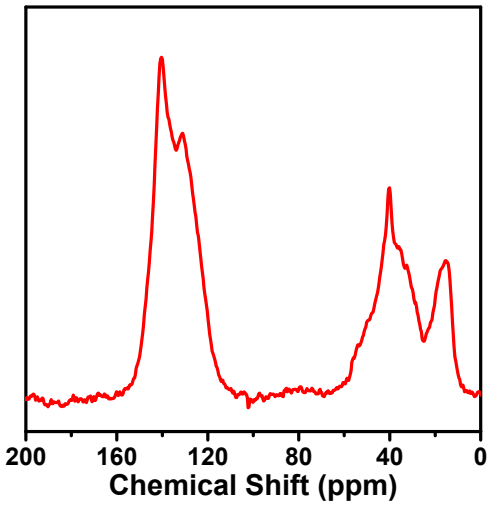

Figure S2. Solid-state ^{13}C CP/TOSS NMR spectra of NOP-Ad-1.

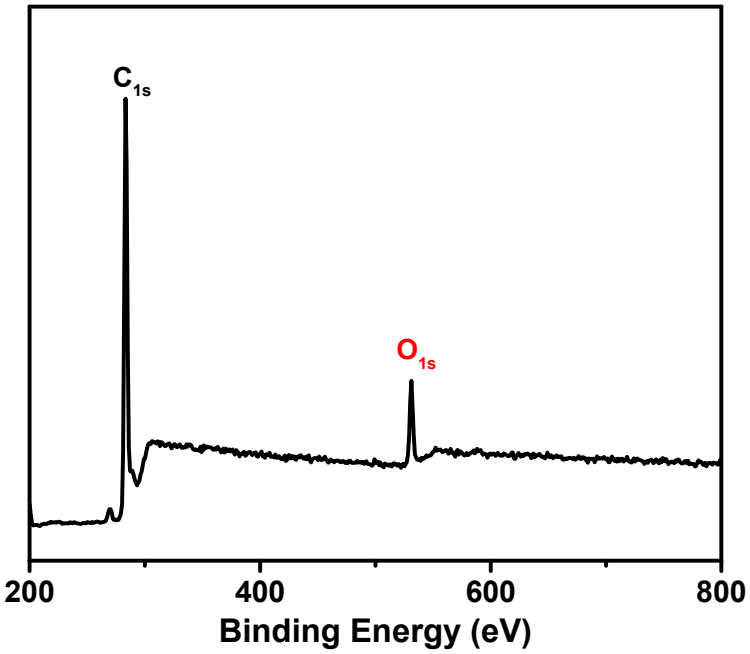

Figure S3 High resolution XPS survey spectra of NOP-Ad-1.

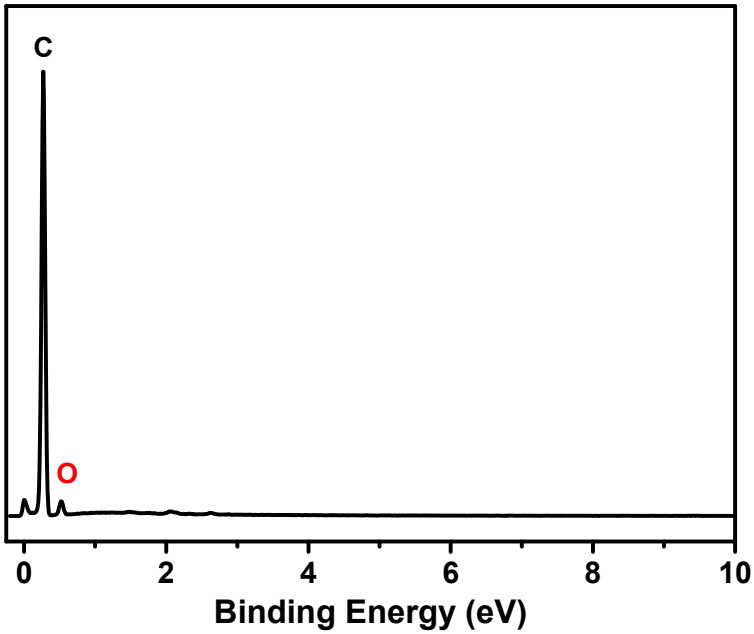

Figure S4. EDX patterns of NOP-Ad-1.

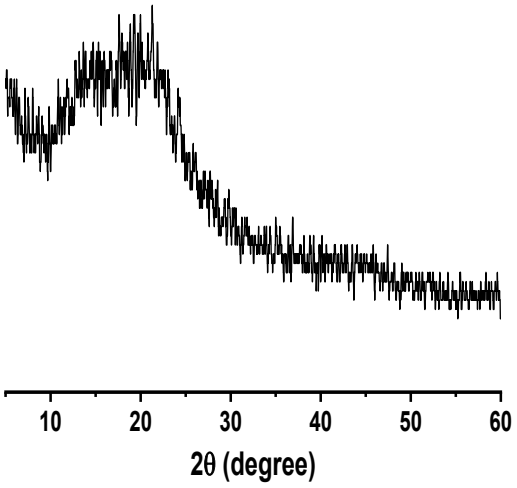

Figure S5. X-ray diffraction of NOP-Ad-1.

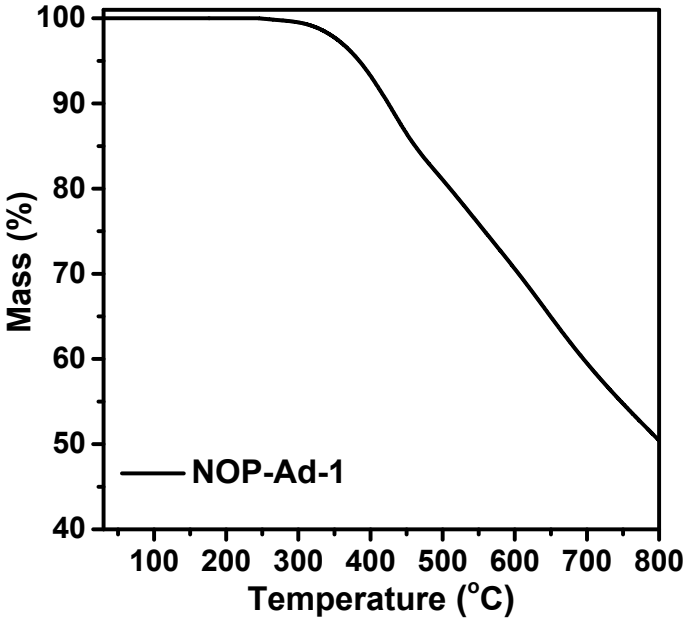

Figure S6. TGA curve of NOP-Ad-1

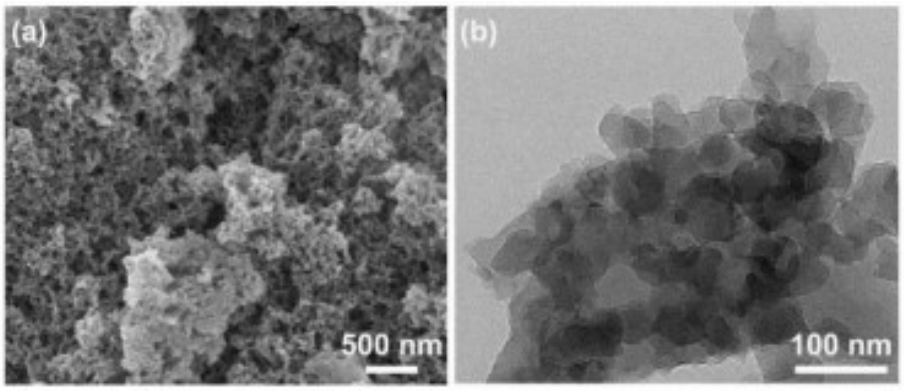

Figure S7. FE-SEM (a) and HR-TEM (b) images of NOP-Ad-1.

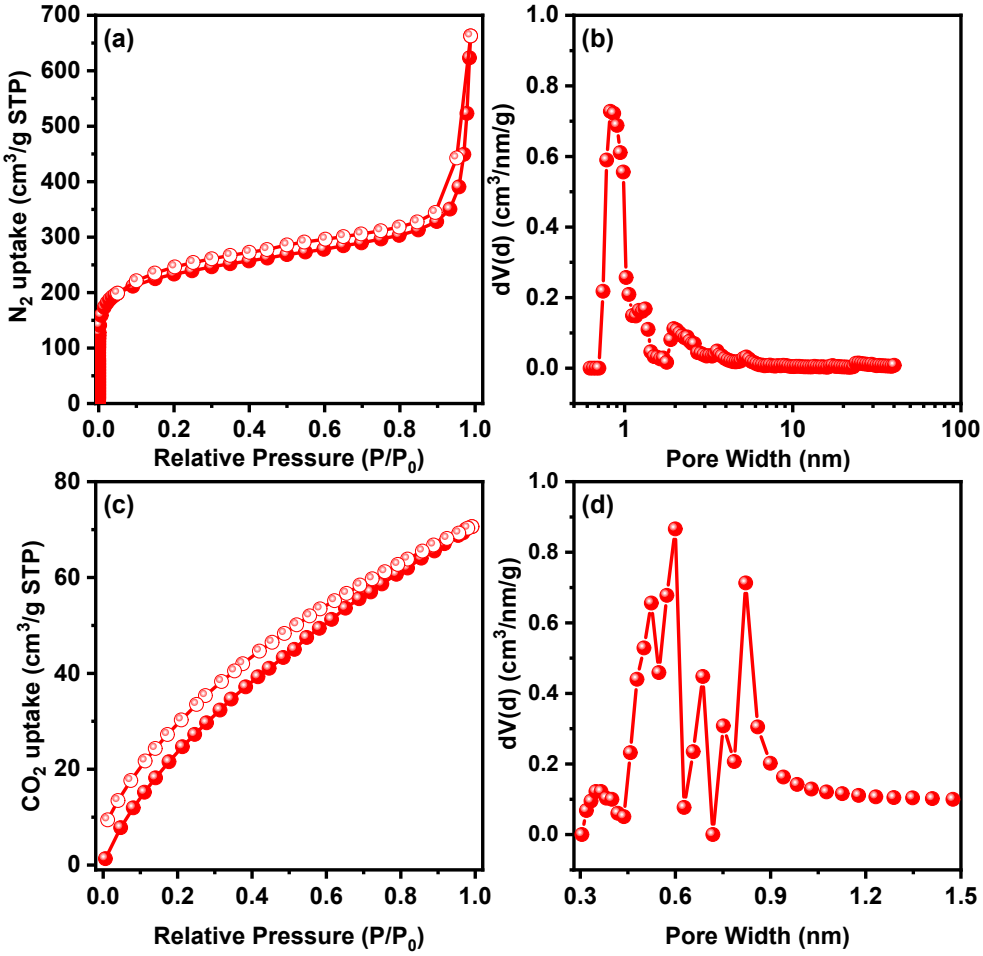

Figure S8. Specific surface area testing of the NOP-Ad-1: (a) N_2 adsorption and desorption isotherms obtained at 77 K; (b) Pore size distribution curves calculated based on NLDFT derived

from N_2 adsorption isotherm at 77 K; (c) CO_2 adsorption and desorption isotherms obtained at 273 K; (d) Pore size distribution curves calculated based on NLDFT derived from CO_2 adsorption isotherm at 273 K.

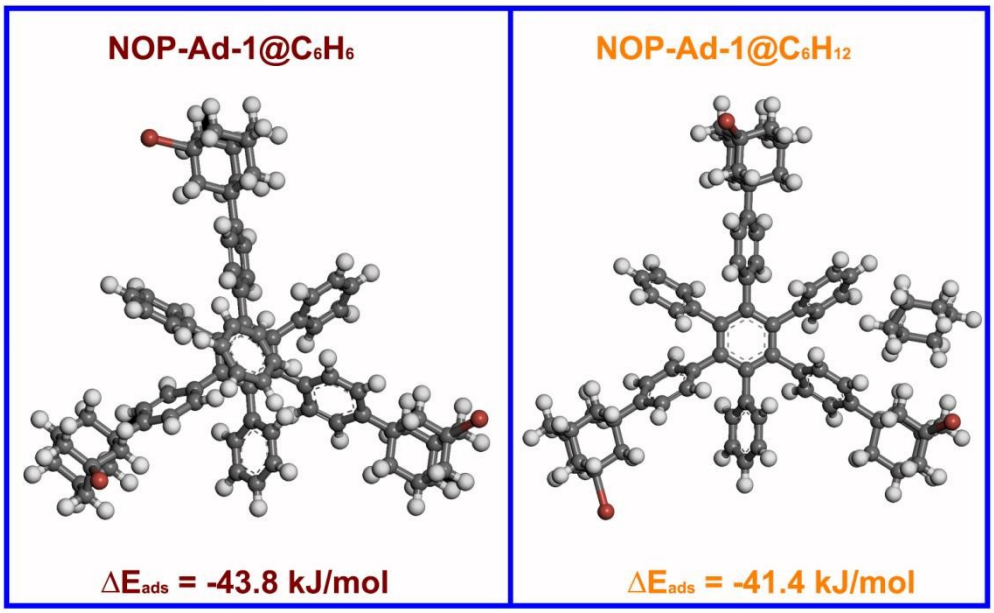

Figure S9. Optimized geometries of the complexes of NOP-Ad-1@C_6H_6 and NOP-Ad-1@C_6H_{12} using Gaussian software.

Table S1. Comparison of uptakes of benzene and cyclohexane vapors, ideal Bz/Cy selectivity between NOP-Ad-1 and other porous materials reported in the literature.

Samples	S_{BET} (m^2/g)	Bz (mg/g)	Cy (mg/g)	Ideal Bz/Cy Selectivity	Ref
NOP-Ad-1	857	989	441	2.24	This work
PAF-2	891	138	7	19.71	1
Hybrid[3]arene	0.9	80.4	7.5	10.72	2
MALP-1	1179	585	492	1.19	3
MALP-2	1126	545	472	1.15	3
MALP-3	1141	571	488	1.17	3
MALP-4	1093	558	465	1.20	3
PAN-1	925	726	527	1.38	4
PAN-2	1242	692	383	1.81	4
PAN-F	702	544	433	1.26	5
PAN-T	795	570	518	1.10	5
CMP-S-1	873	647.4	378	1.71	6
MP1	1020	765	440	1.74	7
PCN-AD	843	980	574	1.71	8
PBI-Ad-1	1023	980	536	1.83	9
PBI-Ad-2	926	765	463	1.65	9
PCN-TPC	686	176	74	2.38	10
PCN-TPPC	662	778	107	7.27	10
UMC-600	1980	663	527	1.26	11
UMC-700	2212	735	605	1.21	11
UMC-800	2406	868	734	1.18	12
FJU-P6	1066	630.4	313.6	2.01	12
FJU-P7	1425	768.6	640.4	1.20	12
PCN-TA	721	1009	206	4.90	13
PCN-TC	674	867	244	3.55	13
PCN-DC	393	635	129	4.92	13
POP-1	486	1020	658	1.55	15
MPI-1	1454	1198	501	2.39	14
MPI-2	814	766	448	1.71	14
MPI-3	586	549	415	1.32	14
sPI-1	1108	1597	851	1.88	15
sPI-2	900	1760	778	2.26	15
CCTF-1	512	878	441	1.99	16
CCTF-2	538	650	311	2.09	16
CCTF-3	207	136	61	2.23	16

Table S2. The initial flow time, saturation adsorption uptake and selectivity of Bz and Cy based on the breakthrough curve.

Samples	Bz:Cy	Bz		Cy		Bz/Cy Selectivity
		t (s)	uptake (mg/g)	t (s)	uptake (mg/g)	
NOP-Ad-1	20:80	2970	45.74	1492	103.61	1.75
	35:65	2193	66.20	1582	72.36	1.71
	50:50	1815	96.63	1727	62.01	1.56
	65:35	1904	116.82	1688	41.54	1.51
	20:80	2517	145.25	2326	28.78	1.24

Table S3. The static adsorption uptake and ideal selectivity of Bz and Cy based on the adsorption isotherm at 298 K.

Samples	Relative Pressure (P/P_0)	Bz uptake (mg/g)	Cy uptake (mg/g)	Ideal Bz/Cy Selectivity
NOP-Ad-1	0.20	394.2	280.9	3.76
	0.35	482.3	322.3	2.31
	0.50	560.7	358.5	1.56
	0.65	632.5	388.5	1.06
	0.80	716.3	419.6	0.64

Reference

1. H. Ren, T. Ben, E. Wang, X. Jing, M. Xue, B. Liu, Y. Cui, S. Qiu and G. Zhu, *Chem. Commun.*, 2010, **46**, 291-293.
2. J. Zhou, G. Yu, Q. Li, M. Wang and F. Huang, *J. Am. Chem. Soc*, 2020, **142**, 2228-2232.
3. M. Rong, L. R. Yang, L. Wang, H. F. Xing, J. M. Yu, H. N. Qu and H. Z. Liu, *Ind. Eng. Chem. Res.* , 2019, **58**, 17369-17379.
4. G. Y. Li, B. Zhang, J. Yan and Z. G. Wang, *Macromolecules*, 2014, **47**, 6664-6670.
5. G. Li, B. Zhang, J. Yan and Z. Wang, *Chem. Commun.*, 2016, **52**, 1143-1146.
6. T. Chen, W. Zhang, B. Li, W. Huang, C. Lin, Y. Wu, S. Chen and H. Ma, *ACS Appl. Mater. Interfaces* 2020, **12**, 56385-56392.
7. X. Ma, Y. Wang, K. Yao, Z. Ali, Y. Han and I. Pinnau, *ACS Omega*, 2018, **3**, 15966-15974.
8. C. Shen, H. Yu and Z. Wang, *Chem. Commun.*, 2014, **50**, 11238-11241.
9. B. Zhang, G. Y. Li, J. Yan and Z. G. Wang, *J. Phys. Chem. C*, 2015, **119**, 13080-13087.
10. G. Deng and Z. Wang, *ACS Appl. Mater. Interfaces*, 2017, **9**, 41618-41627.
11. J. Yan, B. Zhang and Z. Wang, *J. Phys. Chem. C* 2017, **121**, 22753-22761.
12. L. Chen, H. Zhang, Y. Ye, Z. Yuan, J. Wang, Y. Yang, S. Lin, F. Xiang, S. Xiang and Z. Zhang, *New J. Chem.*, 2021, **45**, 22437-22443.
13. C. J. Shen, J. Yan, G. Y. Deng, B. A. Zhang and Z. G. Wang, *Polym. Chem.*, 2017, **8**, 1074-1083.
14. G. Y. Li and Z. G. Wang, *Macromolecules*, 2013, **46**, 3058-3066.
15. J. Yan, B. Zhang and Z. Wang, *Polym. Chem.*, 2016, **7**, 7295-7303.
16. J. Yan, H. Y. Sun, Q. L. Wang, L. Lu, B. Zhang, Z. G. Wang, S. W. Guo and F. L. Han, *New J. Chem.*, 2022, **46**, 7580-7587.